IMAGE

Imagery in Life Sciences

The Challenges of MRI

Techniques and Quantitative Methods for Health

Coordinated by
Hélène Ratiney
Olivier Beuf

ISTE

WILEY

The Challenges of MRI

SCIENCES

Image, Field Director – Laure Blanc-Féraud

Imagery in Life Sciences, Subject Head – Françoise Peyrin

The Challenges of MRI

Techniques and Quantitative Methods for Health

Coordinated by
Hélène Ratiney
Olivier Beuf

ISTE

WILEY

First published 2024 in Great Britain and the United States by ISTE Ltd and John Wiley & Sons, Inc.

ISTE Ltd
27-37 St George's Road
London SW19 4EU
UK

www.iste.co.uk

John Wiley & Sons, Inc.
111 River Street
Hoboken, NJ 07030
USA

www.wiley.com

Library of Congress Control Number: 2023943624

British Library Cataloguing-in-Publication Data
A CIP record for this book is available from the British Library
ISBN 978-1-78945-113-9

ERC code:
LS7 Applied Medical Technologies, Diagnostics, Therapies and Public Health
LS7_1 Imaging for medical diagnosis

Contents

Introduction

Hélène RATINEY and Olivier BEUF
CREATIS, CNRS, Inserm, INSA Lyon, Université Claude Bernard Lyon 1, France

Since its inception in 1973, magnetic resonance imaging has experienced remarkable technological and methodological advancements. Magnetic resonance imaging (MRI) has reached a certain level of maturity, as well as complexity, where several expertise domains merge: biology, medicine, physical chemistry, physics and computer science. A great number of publications on this topic are aimed at the medical world (radiologists, radiographers), while others describe the physics of MRI and target a wider public, including scientists, from the master level to senior researchers. The present work seeks to cover the techniques and methods considered promising for the future of MRI. These approaches provide data way beyond the anatomical structure, including functional, hemodynamic, structural, biomechanical or even biochemical information. Retrieving each of these kinds of data requires understanding and describing a physical phenomenon and putting this knowledge into practice by drawing upon the areas of engineering and, in particular, signal and image processing.

This work thus strives to describe the practical implementation of a great variety of techniques by recalling the underlying physics and by giving details of the modelization and analysis that enable acquisition strategies and retrieval informations. The authors approached the challenge of providing in each chapter the keys to a general overview of a technique or domain by following summarized formulations and citing bibliographic references considered the most relevant. Indeed, each chapter's topic could be covered in a separate book in order to completely satisfy the authors' pedagogic goal. Whether the reader is a master's or

The Challenges of MRI,
coordinated by Hélène RATINEY and Olivier BEUF.

doctoral student, a researcher in medical imaging or a staff member at a university hospital, they will find in this work the information necessary for understanding multiparametric MRI and today's challenges in the field of MRI.

In the first four chapters, this work covers the fundamental notions and principles, deemed useful in MRI, in a brief but sometimes new way. Chapter 1 describes the basics of an MRI scan and the related instrumentation signal chain while introducing the notion of quantification. A special overview is dedicated to the radiofrequency coils used for the excitation and reception of MRI signals in Chapter 2. In Chapter 3, the main acceleration techniques for fast imaging are described along with citations of the most recent methods. Chapter 4 covers the basics of diffusion MRI. Chapters 5–8 are dedicated to a group of MRI techniques for probing or characterizing tissues and organs in vivo. These include functional imaging (Chapter 5), vascular imaging (Chapter 6), quantitative elastography imaging (Chapter 7), magnetization transfer and ultra-short echo-time imaging (Chapter 8), in vivo nuclear magnetic resonance (NMR) spectroscopy and chemical exchange saturation transfer (CEST) imaging (Chapter 9). Chapter 10 presents some novel methods which provide multiple parameters using a single sequence by combining fast acquisition techniques and advanced data processing. Finally, the last two chapters cover a broader overview by describing the state-of-the-art techniques and challenges in interventional MRI in Chapter 11 and ultra-high-field MRI in Chapter 12.

All the co-authors are members of the French Society for Magnetic Resonance in Biology and Medicine (Société française de résonance magnétique en biologie et médecine – SFRMBM) and this work represents an educational contribution of this community stemming from and disseminating for scientific research.

1

MRI Principles, Hardware Components and Quantification

Hervé SAINT-JALMES[1], Hélène RATINEY[2] and Olivier BEUF[2]

[1] *LTSI, Inserm, Université de Rennes, France*

[2] *CREATIS, CNRS, Inserm, INSA Lyon, Université Claude Bernard Lyon 1, France*

1.1. Introduction

The demonstration of the nuclear magnetic resonance (NMR) phenomenon in condensed matter in 1946 (Bloch 1946; Purcell et al. 1946) certainly stems from significant progress accrued during the previous decade and in particular during the war with the development of radars and radiofrequency technology. Today, a similar consideration can be made for magnetic resonance imaging (MRI), where technological progress contributes significantly to the improvement of measurement instrumentation and therefore to the quality of signal and images produced by these devices. Such progress paves the way for imaging techniques that are not exclusively qualitative but also quantitative.

This introductory chapter concisely describes MRI principles and the main components of an MRI scanner, in particular those responsible for the generation of magnetic fields and signal acquisition.

Schematically, several steps are required to obtain a localized spectrum or an image (see Figure 1.1):

For a color version of all the figures in this chapter, see www.iste.co.uk/ratiney-beuf/challenges.zip.

The Challenges of MRI,
coordinated by Hélène RATINEY and Olivier BEUF.

1) the system of spins in a sample must reach thermal equilibrium, which leads to a macroscopic magnetization M_0 being produced in the presence of a static polarization field B_0;

2) the equilibrium of the macroscopic magnetization is perturbed by tilting the M_0 vector away from its equilibrium position by means of a radiofrequency magnetic field B_1;

3) spatial encoding is performed using magnetic field gradients;

4) the system's response following the perturbation is observed by gathering the MR signal by means of a radiofrequency coil;

5) the spectrum or image is reconstructed and quantitative parameters are extracted.

In the following, we will focus on recalling the physical principles of MRI along with the associated technological solutions and their implementation (Saint-Jalmes 2022) up to a general overview of quantitative MRI approaches that are amply presented in this book.

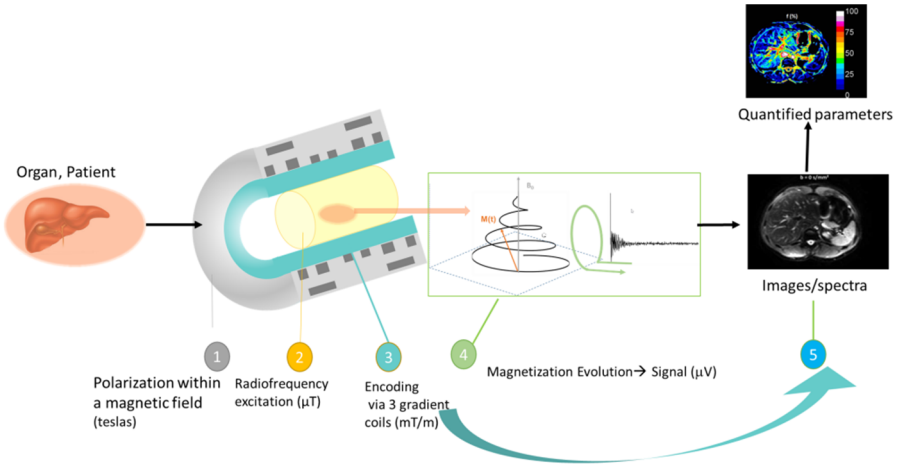

Figure 1.1. *Sequence of four key steps of an MRI scan of an organ, with a fifth step of image/spectrum reconstruction and extraction of quantified parameters*

In NMR and MRI, the denomination of magnetic field ***B*** is commonly used. From a physical point of view, ***B*** is a fundamental quantity, similar to the electric field ***E*** in electrostatics (Gié et al. 1976). In the past, the mathematical analogy between vectors ***E*** and ***H*** led to ***H*** being called the magnetic field, with ***B*** being then

referred to as magnetic induction. The latter term will not be used in this work, although it is still widely used.

1.2. Macroscopic magnetization and static magnetic field B_0

1.2.1. *Nuclear magnetization*

NMR makes use of the magnetic properties of nuclei having a non-zero spin h$\boldsymbol{I}$. Among nuclei with such a feature, the most commonly studied are the hydrogen nucleus (^{1}H or proton), phosphorus-31 (^{31}P), sodium-23 (^{23}Na), fluorine-19 (^{19}F) and carbon-13 (^{13}C) (see Chapter 9). In a nucleus with a spin number I (integer or half-integer), the magnetic nuclear moment $\boldsymbol{\mu}$ is aligned with the spin moment, such that $\boldsymbol{\mu} = \gamma\hbar\boldsymbol{I}$, where γ, called the gyromagnetic ratio, is a characteristic constant of the nucleus of interest and $\hbar$ is the reduced Planck's constant $h/2\pi$ with $h = 6.62 \times 10^{-34}$ J.s.

Whenever a sample with a large number N of identical nuclei having spin number I is subjected to a magnetic field $\boldsymbol{B_0}$, it possesses a resulting magnetization vector $\boldsymbol{M_0}$ according to the Boltzmann equation:

$$\boldsymbol{M_0} = \frac{N\gamma^2\hbar^2 I(I+1)}{3k_B T}\boldsymbol{B_0} \qquad [1.1]$$

where k_B is the Boltzmann constant ($k_B = 1.38 \times 10^{-23}$ J.K^{-1}) and T the absolute temperature. At thermal equilibrium, the macroscopic magnetization $\boldsymbol{M_0}$ has only one longitudinal component oriented along $\boldsymbol{B_0}$, which can be expressed as $\boldsymbol{M_0} = \chi_0 \boldsymbol{B_0}$, where χ_0 is the nuclear magnetic susceptibility. This nuclear magnetization, the evolution of which is inversely proportional to temperature T, is extremely small (typically of 4.8 pA/m for 1 mm^3 of water at 1.5 T and $T = 300$ K) (Abragam 1961).

1.2.2. *Magnet*

An MRI system is similar to a chain: the weakest component determines the final performance of the entire system. In this regard, a significant role is played by the magnet as its choice and features directly influence image quality together with the purchase and operations costs of an MRI device.

1.2.3. *Roles and orders of magnitude*

The static magnetic field is employed both for polarizing the sample and imposing the frequency of excitation and signal acquisition. These two aspects

determine the specifications and constraints of the magnet. In the remainder of this chapter, we shall limit ourselves to the description of devices for clinical imaging; nevertheless, most of the arguments are largely transposable to preclinical imaging (i.e. imaging used in animal model studies).

1.2.3.1. *Field strength*

Performing medical MRI scans at fields lower than a tenth of a tesla seems difficult since the field should be sufficiently high in order to produce an image with an acceptable spatial resolution within a reasonable acquisition time. Indeed, the lower the field, the lower the signal is, and therefore the signal-to-noise ratio (S/N) is low.

By increasing the field strength, S/N is increased and therefore the spatial resolution and/or the scan time is reduced (a trade-off between the two always exists). However, the higher the field, the more challenges arise related to the propagation of radiofrequency waves and safety aspects (see Chapter 12). Furthermore, the cost of a magnet and that of the entire MRI scanner increase significantly with field strength. Thus, magnets with fields higher than 3 T are seldom encountered in clinical routine, with ultra-high-field magnets nowadays typically built to satisfy research needs. Finally, regulations (2013/35/UE) describe the minimal safety indications for the staff exposed to magnetic fields.

1.2.3.2. *Volume of interest, spatial uniformity and temporal stability*

The strong magnetic field (between a few tenths of a tesla and a few teslas) has to be induced over a volume of interest (e.g. tens of liters in clinical imaging) while allowing the scanned body to access the center of the magnetic field region.

In order to produce a spatially well-resolved image or a fine spectrum, the magnet's B_0 field must be as uniform (or homogeneous) as possible over the volume of interest. For whole-body imaging, uniformity of the order of a part per million over volumes of several tens of liters is sought. As an example, in a field of 1.5 T, 1 ppm corresponds to a tiny field variation of 1.5 μT. At the same time, extremely high stability of the field, of the order of 0.1 ppm, is expected over the duration of an exam (between 30 min and 1 h).

1.2.4. *Technical approaches*

To create such a magnetic field, several approaches are available. One of these consists of using the magnetic energy stored in a permanently magnetized material, a magnet. Magnetic fields of the order of tenths of a tesla can be created using ferrites or NdFeB. The shape of the magnet and/or polar ferromagnetic parts can

channel the magnetic flux for a uniform distribution inside the region of interest. The undeniable advantage of this approach is the absence of energy sources. On the other hand, the magnet's mass is considerable (e.g. about ten tons for a field of 0.3 T). In addition, the field intensity in such magnets varies noticeably with temperature (typically 0.1 %/°C). The race toward higher fields has certainly made this approach marginal, although it offers several advantages.

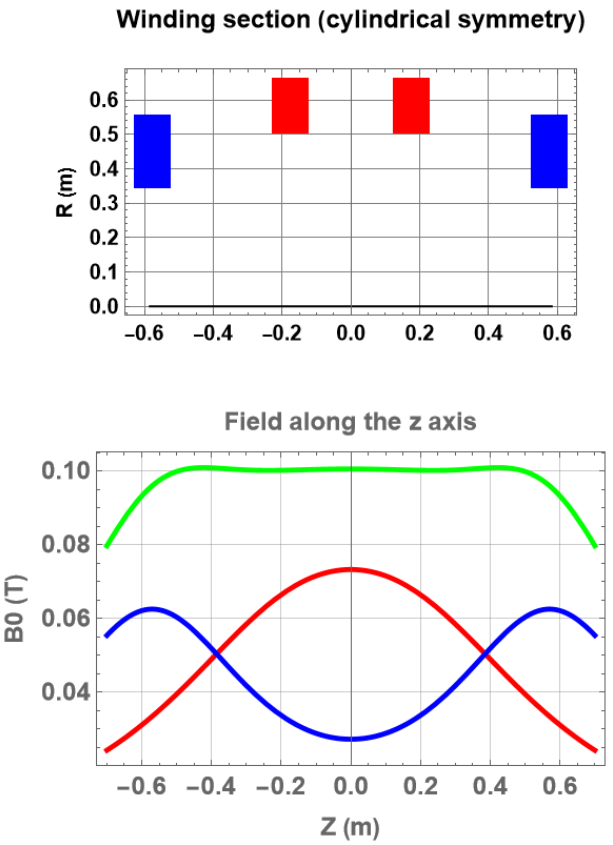

Figure 1.2. *Magnet with two pairs of coils (axisymmetric around the z-axis) and representation of the magnetic fields created along the symmetry axis of the magnet. The two red coils create a strong field at the center of the magnet, together with a significant second-order component (red curve). When the blue pair of coils are added, despite being less efficient, they produce a negative second-order component (blue curve) which can compensate for the imperfection and provide a uniform field (green curve)*

The most widely employed approach consists of a constant direct current flowing in a conducting or superconducting material. The superconducting approach is unavoidable for creating strong fields used for clinical imaging.

The design of the first MRI magnets was based on the pioneering work by Garrett in the 1950s. Garrett was the first person to solve the magnet design problem (Garrett 1951) by expressing the field distribution in the form of zonal harmonics. For this series, the goal consists of canceling as many components as possible up to the 12th, 16th or even 20th order via compensations between different coils, such that only the constant component B_0 remains dominant. This principle is illustrated in Figure 1.2.

1.2.4.1. *Physical size (imaging volume, length, diameter)*

The scanned volume with a uniform field has to be sufficiently large to accommodate the body part to be scanned. In practice, the magnet volume has to be larger than that, since patient access must be possible in a magnet for medical imaging. Patient comfort is an additional challenge. A typical imaging volume in clinical systems is a sphere or an ellipsoid of about 45–55 cm in diameter. The minimum length of the magnet is constrained by the field homogeneity requirement. However, from a patient's point of view, a shorter magnet is better, since the claustrophobic feeling during an imaging scan can be consequently reduced. Typically, the magnets employed in clinical systems have a minimum total length (i.e. including the cryostat) between 150 cm for a 1.5 T field and about 300 cm for 7 T. At the same time, the diameter of the magnet has to be as large as possible for patient access. On the other hand, for a given performance, the cost of the magnet and its footprint increase very rapidly with its diameter.

1.2.4.2. *Installation site requirements*

Among other constraints, the magnet has to meet its siting requirements, taking into consideration aspects such as the footprint, mass and shielding. One of the main concerns is the magnet's fringe field: although the magnetic field targets the center of the magnet (e.g. for a value of 1.5 T), it extends beyond the magnet's boundaries, which may cause problems in a hospital environment. For security reasons, the location of the 0.5 mT or 5-gauss (1 T = 10,000 G) line is considered. This field limit was defined in the early days of MRI to guarantee the safe operation of cardiac stimulators. Any access to the area where B_0 is higher than 0.5 mT must be controlled and notified by panels, such as ones that read "Caution – strong magnetic field". Thus, there is a need to shield the magnet to restrict this "0.5 mT area" as much as possible. This is an important aspect in practice because the hospital obviously seeks to use the smallest rooms possible. The fringe field in a non-shielded 1.5 T magnet extends in three spatial directions up to about ±10 m

along the field direction and ±7 m in the other directions; this means that a 300 m^2 room is required to site the magnet, which is not very realistic. Therefore, some kind of shielding is inevitably necessary. The shielding can be passive or active.

The first possible idea for shielding for fringe field suppression is to add iron beams. However, the magnet mass increases significantly and an accurate calculation of the magnetic field becomes very challenging due to the strongly nonlinear behavior of the materials.

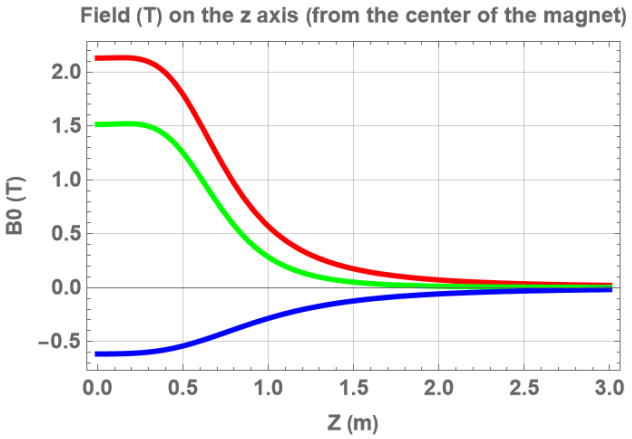

a)

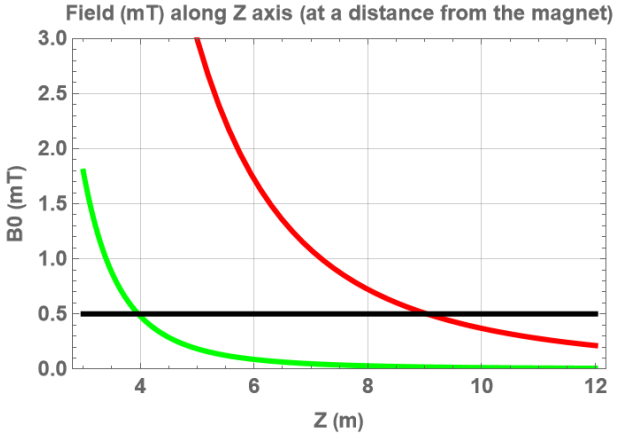

b)

Figure 1.3. *The field produced by the coils is the strongest at the center of the magnet (red curve a), but it is also strong outside the magnet (red curve b)*

COMMENT ON FIGURE 1.3.– *The 0.5 mT line (straight black curve, b) is located at 9 m from the center of the magnet. If coils with opposite currents are added, the field strength at the center is reduced (blue curve, a), but the resulting field (green curve, b) makes the 0.5 mT line located 4 m from the magnet center. For that, in this example, a 2 T field and an opposing 0.5 T field have to be produced to obtain a 1.5 T field at the magnet center*.

Active shielding was introduced at the end of the 1980s. In this approach, shielding coils with a diameter larger than the main magnet carry a current with the opposite orientation with respect to the main magnet coils' current. The effect of such a configuration on the fringe field is shown in Figure 1.3. In this way, the field produced outside the magnet (fringe field) is significantly reduced. This approach increases the magnet cost not only because of a larger number of coils but also because the field produced by the main magnet coils is reduced at the center of the scanner by the shielding coils. Consequently, the number of turns of the main magnet coils has to be increased to compensate for the significant decrease in field strength at the magnet center. The magnet complexity increases and the design process becomes longer since minimizing the 0.5 mT area introduces an additional constraint to the optimization process. Nevertheless, active shielding also has great advantages, being a solution that is lightweight and not dependent on the environment of the magnet.

1.2.4.3. *Costs*

The fabrication and operation costs of a magnet are high. These costs are related to the magnetic energy E_s stored in the magnet. In general, for resistive and superconducting magnets, $E_s \sim B_0^2 V$, where V is the accessible patient volume. Therefore, increasing the field B_0 or increasing the volume corresponds to increasing the magnetic energy, and thus an increase in costs, even though the latter consequence is indirect. For example, by increasing the field from 0.3 T to 1.5 T, the required energy is multiplied by 25 and reaches several MJ in a 1.5 T magnet for clinical imaging use.

1.2.4.4. *Typical superconducting magnet for MRI*

A typical magnet for a clinical MRI scanner creates a magnetic field of 1.5 T or 3 T. For such field values, the only possible technology today consists of superconductors. Once a wire made of NbTi is immersed in liquid helium at 4.2 K, this wire does not oppose any resistance to current flow, at least if critical current density and maximum field values along the wire are not reached. Hence, the entire coil has to be drowned in liquid helium, which requires a volume of the order of a thousand liters. Additionally, due to the temperature gradient between the helium

and the magnet's outside, rather elaborate cryostats have to be used to limit helium leakage as much as possible. Currently, a cryo-cooling system employing a cold head can avoid wasting helium, which is a non-renewable and expensive element; however, the operation of such systems requires electrical power. In the vast majority of MRI scanners, the magnet has a cylindrical shape, which is motivated by the constraints described earlier: homogeneity over the volume of interest, patient access to the region with a homogeneous field and costs minimization. Patient access is achieved via a tunnel of 60 or 70 cm in diameter. Today, the typical length of the magnet is between 150 cm and 200 cm for these field strengths (1.5 T and 3.0 T). This leads to coils built following a cylindrical shape of about 1 m in diameter. In a superconducting magnet, the magnetic field inside the coil wires has to be evaluated, as well as the magnetic forces between them. The main constraints are thus an acceptable current density within the wire and reasonable geometrical size and position of the coils inside the magnet. All the primary coils are located on the same support; otherwise, the cryogenic system becomes too large to be practical and/or the supporting mechanical structure becomes too complex. For this reason, the radii of the various coils should not differ too much (a few percent). An integer number of turns is defined for each coil, enabling all the magnet coils to be connected in series. The magnet includes a dozen coils, plus active shielding. A typical example of such a structure providing a homogeneity of 1 ppm over a spherical volume of 50 cm in diameter is given in Figure 1.4.

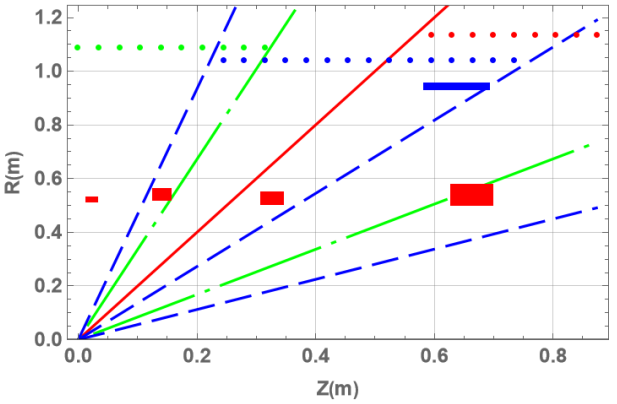

Figure 1.4. *Example of a magnet structure for clinical MRI with a field of 1.5 T*

COMMENT ON FIGURE 1.4.– *The figure employs a quadrant representation: the magnet is symmetrical with respect to the vertical axis, and the cylindrical coils with axial symmetry around the Z-axis are represented by their red and blue sections. The magnet is composed of four coil pairs (red sections) wired on a cylinder and*

one pair of coils (blue sections with an opposing field, see Figure 1.3) that significantly reduces the extension of the 0.5 mT line. Magnet optimization is performed globally and we can observe that the reduced coordinate of the coils (Z/R) reduces the z harmonics of the field. The zeros of the latter are represented in red for the second order, in green for the fourth order and in blue for the sixth order.

Once an appropriate architecture is defined, the other elements required for the magnetic system design have to be considered for the construction of the magnet. In a superconducting magnet, once the magnetic forces acting between the different magnet coils have been evaluated during the mechanical drawing phase, the mechanical tools and the support structure must be designed so that they minimize the coil movements during the magnet's cooling down and later when the magnet's field is ramped up. For instance, a magnet designed for a 1 ppm homogeneity can present a variation of the magnetic field of the order of hundreds of ppm once built. The best achievable values one can hope to get after assembly are of the order of 300–400 ppm. This variation can be partially compensated by using dedicated coils (*shim coils*) inserted into the magnet or via calibrated ferromagnetic parts placed with great precision around the internal surface of the magnet. However, compensating for a variation greater than ~2,000 ppm is impossible. Therefore, it is worth taking into account the influence of these variations during the design of a magnet such that, once built, it will be relatively close to the desired performance and sufficiently adjustable.

1.2.4.5. *Compensation or "shim" coils*

Once the magnet is ramped to the target field, the adjustments described above are usually insufficient for reaching a target homogeneity. Approximatley 10 supplementary compensation coils are added for that purpose. The main role of these coils conveying low currents (of the order of a few amperes) is dynamic field correction, an approach that is particularly useful for localized spectroscopy studies (Juchem and De Graaf 2017).

1.2.5. *Novel technologies*

Many new directions are being explored in addition to the development of ultra-high-field magnets. One of these consists of the development of magnets that employ no or very little helium. Indeed, this gas is non-renewable and its cost has increased significantly over the last decades. MRI is actually one of the main consumers of this resource. Permanent magnets are interesting in this sense for creating fields of a few tenths of tesla (see section 1.2.4) and, additionally, they do

not require electrical power. For superconducting approaches, the implementation of NbTi coils cooling via conduction from a cold source in a cryocooler is reaching the market after many technological challenges (vibration minimization, helium-storing thermal buffers with a volume of tens of liters, etc.) have been solved, at least partially. These approaches are more feasible at low to medium fields (≤1.5 T) and many manufacturers offer these kinds of systems with magnetic fields between 0.55 and 1.5 T. Compared with NbTi, cooling is significantly simpler for superconducting materials with a high critical temperature (39 K for MgB_2, over 90 K for mixed oxides of barium, copper and rare-earth elements). However, several limiting aspects remain: above all, the material cost, but also the manufacturing cost of long-length wires required in MRI and the production of controlled systems for transitioning between the superconducting and the conducting states (Parizh et al. 2017). In recent years, such magnets based on MgB_2 or mixed oxides of barium, copper and rare-earth elements have been appearing on the market. Of course, all things being equal, using lower fields considerably simplifies manufacturing and reduces the cost of the magnet. Several researchers have seemingly rediscovered a medical and economic interest in magnetic fields of a few tenths of tesla (Campbell-Washburn et al. 2019). The decrease in S/N in such scanners is compensated by, without any particular order, a decrease in power deposited in the patient and acoustic noise, a very notable reduction of image artifacts, such as those of susceptibility, a larger inner diameter of the scanner (Marques et al. 2019), interventional imaging possibilities, etc.

1.3. Description of the magnetization evolution

In general, understanding NMR phenomena requires quantum physics formulations, but most of these phenomena can still be explained using classical descriptions. In particular, the Bloch model describes the classical fundamentals of most MRI scans.

The evolution of the nuclear magnetization $\boldsymbol{M}$ in the presence of a magnetic field $\boldsymbol{B}$ is described by the phenomenological Bloch equations:

$$\frac{d\mathbf{M}}{dt} = \gamma \mathbf{M} \wedge \mathbf{B} - \frac{M_x \mathbf{i} + M_y \mathbf{j}}{T_2} + \frac{M_0 - M_z}{T_1} \mathbf{k} \qquad [1.2]$$

where M_x, M_y, M_z are the components of $\boldsymbol{M}$ in an orthonormal reference frame of unit vectors $\boldsymbol{i}$, $\boldsymbol{j}$, $\boldsymbol{k}$. T_1 and T_2 are the two characteristic time constants of the recovery of the magnetization $\boldsymbol{M}$ to its equilibrium position $\boldsymbol{M_0}$ aligned with $\boldsymbol{k}$ and the decay of the magnetization components perpendicular to this direction, respectively.

During excitation, the magnetic field $\boldsymbol{B}$ in equation [1.2] corresponds to the static magnetic field $\boldsymbol{B_0}$ – which is the origin of the macroscopic magnetization as described above – plus a radiofrequency field $\boldsymbol{B_1}$, generally of lower amplitude, which temporarily tilts the magnetization vector. During signal detection, $\boldsymbol{B}$ is composed only of the static field $\boldsymbol{B_0}$. The first term in the Bloch equation describes the rotation of the nuclear magnetization around the magnetic field direction. During excitation, we consider the rotation around the effective field given by B_0 plus B_1 (the latter modulated in amplitude and/or frequency). During signal reception, the macroscopic magnetization motion consists of a precession around $\boldsymbol{B_0}$ with an angular frequency ω, called Larmor frequency, such that $\boldsymbol{\omega_0 = -\gamma B_0}$. The other two terms describe the relaxation phenomena with phenomenologically introduced time constants T_1 and T_2. Without going into details about their cause, these terms are related to the interaction of nuclear magnetic moments with their environment and to their individual evolution in the presence of an external perturbation. The evolution of the transverse magnetization component $\boldsymbol{M_{xy}}$ is due to inter-spin dephasing. Its characteristic time T_2 is thus called the transverse or spin–spin relaxation time. The evolution of the longitudinal component $\boldsymbol{M_z}$ is characterized by T_1, the spin-lattice relaxation time. This longitudinal relaxation corresponds to the energy exchange between the spins contributing to the magnetization and the surrounding lattice in order to return to thermal equilibrium. In general, the radiofrequency field B_1 is applied with a short duration with respect to T_1 (of the order of milliseconds) such that the terms with T_1 and T_2 in equation [1.2] are neglected during excitation. During signal reception, equation [1.2] can be solved to obtain the formulas of the evolution of magnetization components over time:

$$M_{xy}(t) = M_{xy}(0)e^{-t/T_2} \qquad [1.3]$$

$$M_z(t) = M_z(0)e^{-t/T_1} + M_0\left(1 - e^{-t/T_1}\right) \qquad [1.4]$$

where $M_{xy}(0)$ and $M_z(0)$ are the transverse and longitudinal magnetization component values at the initial time, while M_0 is the magnetization value at thermodynamic equilibrium.

1.4. Excitation: perturbing the magnetization

1.4.1. *Principle*

The spins system is perturbed by applying a rotating field B_1 perpendicularly to B_0. This radiofrequency field with an angular frequency ω is generated by an

alternating current circulating within a coil. If the magnetic field B_1 oscillates at the Larmor angular frequency ($\omega_0 = \gamma B_0$), the magnetization is tilted from its equilibrium position and starts precessing around B_1 at the angular frequency $\omega_1 = \gamma B_1$, with such a motion being superposed to the precession around B_0. This synchronization between the characteristic frequency of the spins system and the RF pulse frequency is denoted by the term "resonance" and corresponds to a perturbation of nuclear magnetization. For an RF pulse with a constant amplitude B_1 and duration τ, the tilting or "flip" angle α (in radians) is $\alpha = \gamma B_1 \tau$.

The magnetization tilting RF pulse gives rise to a transverse component of the magnetization vector, as the latter starts rotating at the angular frequency ω_0 around B_0 and induces a measurable electromotive force (emf) in a coil. The decay of the transverse magnetization to equilibrium is observed as a free induction decay signal (FID). In sections 1.5 and 1.7, we shall see how the magnetization relaxation to equilibrium can be modulated to obtain information on spatial localization or tissue composition.

1.4.2. *Transmit coil*

The B_1 field is created via a current oscillating at the Larmor frequency in a coil. This magnetic field pulse, with a duration of the order of milliseconds, has a very low amplitude of only a few μT. In clinical imaging, this field is produced by a large transmit coil (about 70 cm in diameter and 50 cm in length). Although the field amplitude is low, the same cannot be said about the required power and typically radiofrequency amplifiers of several tens of kW power this coil (see Chapter 2). The power deposited inside the patient by this radiofrequency emission is non-negligible and it grows rapidly with frequency and hence with B_0 field strength (see Chapter 2). To limit the dissipated power, quadrature excitation is favored. Moreover, at high frequencies (e.g. >100 MHz for a whole body) and thus at high fields, the electrical properties of biologic tissue (permittivity and resistivity) cause significant inhomogeneity of the excitation performed by a single coil. To tackle this problem, a set of transmit coils with signals of different amplitude and phase are implemented (see Chapter 12), similar to the coil arrays used for several years to improve the reception of the NMR signal.

1.4.3. *Radiofrequency signal reception*

Once the B_1 field has tipped the magnetization to the transverse plane, the magnetization's relaxation to equilibrium via a rotating motion at the Larmor

frequency produces a magnetic flux variation, which can be measured by a radiofrequency detector. In its simplest version, this can be done once again via a coil, which is placed perpendicularly to the direction of the B_0 field. The flux variation generates an alternating voltage in the coil, which is then amplified and demodulated (see Chapter 2). The induced voltage is particularly low, typically of the order of μV, hence the need for amplifying and maximizing the signal with respect to undesired noise in the reception signal chain.

Signal reception can be performed with the same coil that is used for transmission. However, the requirements for these two steps are different. Often, a separate coil with an important feature of high uniformity of the RF field B_1 is used for transmission, and a second coil or probe for the reception, where the main requirement is a high sensitivity and high S/N (see Chapter 2). For a surface coil, these properties increase with decreasing diameter of the coil. A significant improvement in image quality, without reducing the imaging field of view, has been enabled by the introduction of phased arrays (Rœmer et al. 1990), where multiple surface coils collaborate to measure the signal simultaneously.

Various acquisition strategies dedicated to the simultaneous scanning of small animals have been developed starting from this approach (Beuf et al. 2006). While the first coils were designed on rigid support structures and were dedicated to limited anatomical regions, the need for patient comfort and continuity among anatomical regions (e.g. head-neck-spine, thorax-abdomen) spurred the manufacturers to develop flexible and lightweight coils, which can be placed on the patient and around different anatomical regions. The latest evolution in this sense is represented by blanket-like coils called AIR (*adaptive imaging receive*). Today's development efforts are oriented toward coils with flexible conductors (McGee et al. 2018) or with extensible ones (Port et al. 2020), which can be worn close to the body like garments, or even coils based on micro-electro-mechanical systems (MEMS) capable of modifying the loops' geometry or changing the frequency to acquire the signal at different frequencies sequentially (Raki et al. 2020). Doing away with the cable connecting the coils to the receiving system is another development path explored in recent years, which however still encounters challenges due to constraints of power supply and noise level which affect the images (Byron et al. 2017). Intermediate approaches based on optical transmission have been developed to get rid of safety concerns (Memis et al. 2008; Saniour et al. 2017). In preclinical settings, coils cooled down to very low temperatures (*Cryocoils*) using helium gas (of the order of 30–35 K) and dedicated to small-animal imaging have provided significant gains in S/N, on average of the order of 3 for magnetic fields between 4.7 T and 11.7 T (Darasse and Ginefri 2003).